CHEMISTRY OF MATERIALS

Article

pubs.acs.org/cm

Cation-Mutation Design of Quaternary Nitride Semiconductors Lattice-Matched to GaN

Zeng-Hua Cai,[†] Prineha Narang,[‡] Harry A. Atwater,[‡] Shiyou Chen,*[,†] Chun-Gang Duan,[†] Zi-Qiang Zhu,[†] and Jun-Hao Chu[†]

[†]Key Laboratory of Polar Materials and Devices (MOE), East China Normal University, Shanghai 200241, China

[‡]Thomas J. Watson Laboratory of Applied Physics, California Institute of Technology, Pasadena, California 91125, United States

Supporting Information

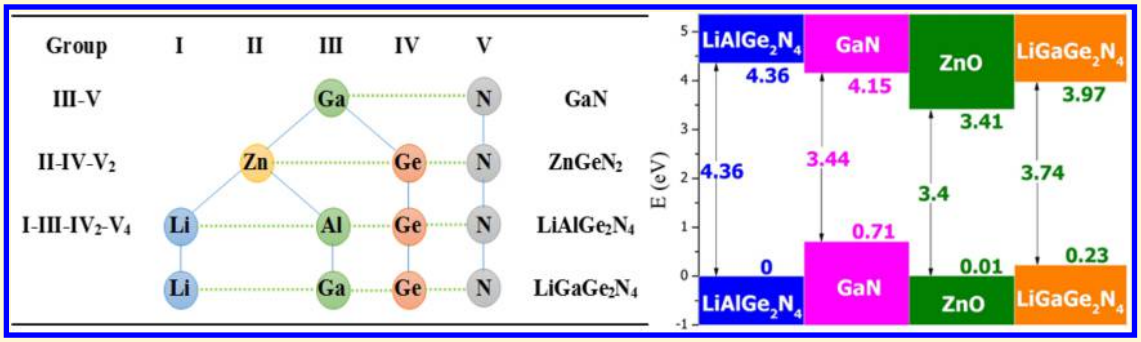

ABSTRACT: The search for new direct bandgap, earth-abundant semiconductors for efficient, high-quality optoelectronic devices, as well as photovoltaic and photocatalytic energy conversion has attracted considerable interest. One methodology for the search is to study ternary and multiternary semiconductors with more elements and more flexible properties. Cation mutation such as binary → ternary → quaternary for ZnS → $CuGaS_2$ → Cu_2ZnSnS_4 and ZnO → $LiGaO_2$ → Li_2ZnGeO_4 led to a series of new quaternary chalcogenide and oxide semiconductors with wide applications. Similarly, starting with GaN, ternary nitrides such as $ZnSnN_2$ and $ZnGeN_2$ have been designed and synthesized recently. However, quaternary nitride semiconductors have never been reported either theoretically or experimentally. Through a combination of the Materials Genome database with the first-principles calculations, we designed a series of quaternary nitride compounds I−III−Ge_2N_4 (I = Cu, Ag, Li, Na, K; III = Al, Ga, In) following the GaN → $ZnGeN_2$ → I−III−Ge_2N_4 mutation. Akin to Li_2ZnGeO_4, these quaternary nitrides crystallize in a wurtzite-derived structure as their ground state. The thermodynamic stability analysis shows that while most of them are not stable with respect to phase separation, there are two key exceptions (i.e., $LiAlGe_2N_4$ and $LiGaGe_2N_4$), which are stable and can be synthesized without any secondary phases. Interestingly, they are both lattice-matched to GaN and ZnO, and their band gaps are direct and larger than that of GaN, 4.36 and 3.74 eV, respectively. They have valence band edges as low as ZnO and conduction band edges as high as GaN, thereby combining the best of GaN and ZnO in a single material. We predict that flexible and efficient band structure engineering can be achieved through forming GaN/$LiAlGe_2N_4$/$LiGaGe_2N_4$ heterostructures, which have tremendous potential for ultraviolet optoelectronics.

I. INTRODUCTION

As a wide-band gap semiconductor, GaN has attracted wide attention for its applications in blue optoelectronic, high-power, and high-frequency devices.[1,2] To engineer the band gap and band structure of GaN for ultraviolet applications, ternary AlGaN ($Al_xGa_{1-x}N$)[3] and quaternary AlGaInN ($Al_xGa_{1-x-y}In_yN$)[4−7] alloys have been synthesized. GaN/AlGaN and GaN/AlGaInN superlattices are grown for multiquantum-well-based ultraviolet light-emitting diodes (LEDs).[8,9] Although this is the most established method to engineer the band structure of GaN-based devices, the composition nonuniformity and the GaN/AlGaInN lattice-mismatch hindered the improvement of device performance.[10] (Note that the homogeneous AlGaInN alloys had been successfully fabricated in recent studies.[5−7])

Cation-mutation is another method for band structure engineering of semiconductors. For example, in ZnS, two Zn^{2+} cations can be mutated into one Cu^+ cation and one Ga^{3+} cation, and then a ternary semiconductor $CuGaS_2$ can be derived. In $CuGaS_2$, two Ga^{3+} can be further mutated into one Zn^{2+} and one Ge^{4+}, and then a quaternary semiconductor Cu_2ZnGeS_4 can be derived,[11,12] as shown in Figure 1. Ge^{4+} can also be substituted by Sn^{4+}, and S^{2-} anion by Se^{2-}, and then a series of I_2−II−IV-VI_4 semiconductors can be derived. Among them, Cu_2ZnSnS_4 and $Cu_2ZnSnSe_4$ have much smaller band

Received: September 9, 2015
Revised: October 31, 2015
Published: November 2, 2015

DOI: 10.1021/acs.chemmater.5b03536
Chem. Mater. 2015, 27, 7757−7764

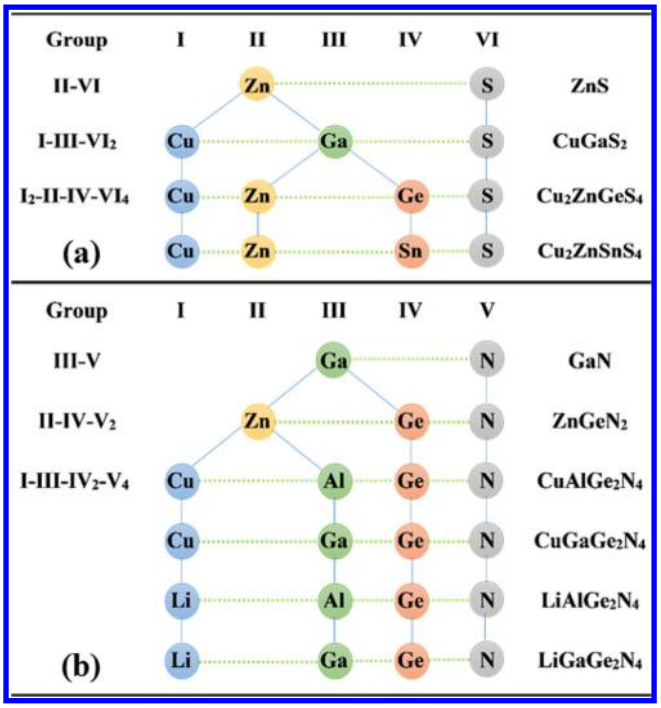

Figure 1. Schematic plot of the cation-mutation design of quaternary chalcogenide (a) and nitride (b) semiconductors, derived from binary II−VI ZnS and III−V GaN, respectively. Cu or Li can also be replaced by other group I (I = Ag, Na, K) cations and Al or Ga by other group III (III = In) cations, and subsequently, 15 quaternary nitrides can be designed.

gaps (1.0−1.5 eV) than ZnS, making them ideal light absorber materials in thin film solar cells.[13−17]

This idea for band structure engineering was proposed by Pamplin and Goodman as early as the 1950s,[18,19] but the concept did not attract intensive attention until recently when new applications have been explored based on these quaternary semiconductors with more flexible properties than binary semiconductors.[20−25] Because there are four chemical elements involved, it becomes possible to tune the lattice constants, band gap, and band edge positions more flexibly; for example, if we design quaternary nitride semiconductors derived from GaN, we may manipulate the band gaps (edges) while fixing the lattice constants to avoid a lattice-mismatch between the quaternary nitrides and GaN, so that their respective superlattices can be easier to grow. On the other hand, it is desirable that the quaternary nitrides crystallize in an ordered structure and not phase-separate at low growth temperature, in contrast with the AlGaN and AlGaInN disordered alloys, which tend to phase-separate at low temperature and require a high deposition temperature to ensure the composition uniformity.

Following this cation-mutation idea (Figure 1b), recently ternary $ZnGeN_2$, $ZnSnN_2$, and their alloys $ZnSn_xGe_{1-x}N_2$ derived from GaN have been designed and also synthesized successfully. Furthermore, their band gaps can be tuned almost linearly from 3.4 to 2.0 eV through changing the Sn/Ge composition.[26,27] As shown in Figure 1b, further mutation of the Zn^{2+} into the group I and III cations is still possible, which will lead to a series of quaternary nitrides I−III−Ge_2N_4. However, these quaternary nitrides have never been reported, either theoretically or experimentally. This is in contrast with the case in sulfides or oxides where a large amount of quaternary compounds such as Cu_2ZnGeS_4, Cu_2ZnSnS_4, Cu_2CdSnS_4, and Li_2ZnGeO_4 have been synthesized with various applications.[16,28−32] It is currently unknown whether these quaternary nitrides can be synthesized. If these quaternaries can be synthesized and their band structure and lattice constants can be tuned with more freedom, they may replace (or compete with) the AlGaN, InGaN, or AlGaInN alloys and form lattice-matched heterostructures with GaN.

In this paper, we show the design of a series of quaternary nitride compounds I−III−Ge_2N_4 (I = Cu, Ag, Li, Na, K; III = Al, Ga, In) following the GaN → $ZnGeN_2$ → I−III−Ge_2N_4 mutation, and we predict their crystal structure and thermodynamic stability based on the first-principles calculations. Most of these nitrides are not stable with respect to phase separation, which explains why the quaternary nitrides have never been reported. There are, however, two key exceptions, $LiAlGe_2N_4$ and $LiGaGe_2N_4$, which are stable and may be synthesized without secondary phases. Interestingly, their lattice constants are well matched to that of GaN, and their band gaps are both larger than that of GaN, with the valence band edge close to that of ZnO and the conduction band edge close to that of GaN. So they could replace (or compete with) the AlGaInN alloys and form lattice-matched GaN/$LiAlGe_2N_4$/ $LiGaGe_2N_4$ superlattices or heterostructures, which would be ideal for ultraviolet optoelectronic devices.

II. DESIGN SCHEME AND CALCULATION METHODS

A schematic plot of the cation-mutation design of the quaternary semiconductors is shown in Figure 1. Similar to the mutation ZnS → $CuGaS_2$ → Cu_2ZnGeS_4 (or Cu_2ZnSnS_4, Ag_2ZnSnS_4), which have been well studied, GaN can also be mutated into ternary $ZnGeN_2$ through mutating the Ga^{3+} (III) cations into the Zn^{2+} (II) and Ge^{4+} (IV) cations, and the $ZnGeN_2$ can be further mutated into $CuAlGe_2N_4$ through mutating Zn^{2+} (II) into Cu^+ (I) and Al^{3+} (III). If the group I and III cations are replaced by I = Cu, Ag, Li, Na, K; III = Al, Ga, In, a series of I−III−Ge_2N_4 (more generally I−III−IV_2-V_4) quaternary nitrides can be derived from the binary GaN.

One major principle in this cation-mutation is that the chemical balance is always maintained, so Ga^{3+} are replaced by Zn^{2+} and Ge^{4+} (their average valence is equal to that of Ga^{3+}), and Zn^{2+} is replaced by Cu^+ and Al^{3+}. This chemical balance should be maintained everywhere in the crystal structure of ternary and quaternary nitrides. In binary GaN, each N^{3-} anion (Ga^{3+} cation) is coordinated by four Ga^{3+} cations (N^{3-} anions), so that it is charge-neutral around each N^{3-} anion (Ga^{3+} cation). After the mutation, each N^{3-} needs to be coordinated by two Zn^{2+} and two Ge^{4+} in $ZnGeN_2$, in order to satisfy the local charge-neutrality condition everywhere in the lattice. Previous studies in the ZnS → $CuGaS_2$ → Cu_2ZnGeS_4 mutation showed that the ordered structures that satisfy this local charge-neutrality condition have lower energies than other structures, which is also known as the octet rule (when the anions are in the eight-electron full-shell state, the structure is energetically more stable).[12] For $ZnGeN_2$, it was also found that the two lowest-energy structures with the smallest primitive cell also satisfy this condition and can be considered as derived from the 16-atom supercell of the GaN wurtzite structure, as shown in Figure 2b,c. For quaternary I−III−Ge_2N_4, two structures that satisfy the local charge-neutrality condition can be derived from the those of $ZnGeN_2$, in which all the cations are ordered and each N^{3-} anion is coordinated by one group I^+, one group III^{3+}, and two Ge^{4+} cations. They have the space group *Pc* (wurtzite-kesterite structure of

DOI: 10.1021/acs.chemmater.5b03536
Chem. Mater. 2015, 27, 7757−7764

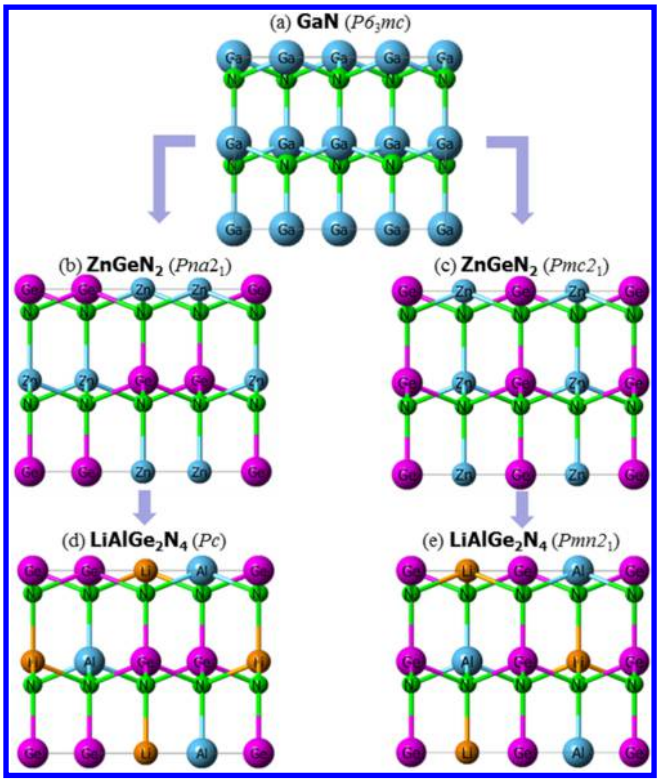

Figure 2. Schematic of the binary GaN in wurtzite structure and $ZnGeN_2$ and $LiAlGe_2N_4$ in wurtzite-derived structures with different symmetry.

Cu_2ZnSnS_4 and Li_2ZnGeO_4[33]) and $Pmn2_1$ (wurtzite-stannite), as shown in Figure 2d,e, respectively. In the following, we will show that they have lower energies than other structures that we considered and are among the low energy structures found using the global crystal structure optimization method.[34,35]

With these quaternary nitride semiconductors designed following the cation-mutation, we studied their crystal structure, electronic and optical properties as well as the thermodynamic stability using the first-principles calculations within the density-functional formalism as implemented in the VASP code.[36,37] For the crystal structure optimization, the exchange−correlation functional that we used is the generalized gradient approximation (GGA) of Perdew−Burke−Ernzerhof (PBE).[38] Meanwhile, the hybrid exchange−correlation functional (HSE) was used to calculate the electronic structure and optical properties, because GGA usually underestimates the band gap for these compounds, whereas the HSE functional predicted the band gaps with better agreement with experimental results for Cu_2ZnSnS_4, $ZnGeN_2$, and GaN.[26,39,40] An energy cutoff of 450 eV was used in all cases, and the 4 × 5 × 5 Monkhorst−Pack k-point meshes[41] for the Brillouin-zone integration of the 16-atom primitive cell. To predict the thermodynamic stability of the quaternary I−III−Ge_2N_4 with respect to phase-separation into elemental phases or binary or ternary compounds, all the possible elemental phases or binary or ternary compounds related to the group I and III, Ge and N elements are searched in the Materials Genome (Materials Project) database,[42] and their formation energies are collected from the database.

III. RESULTS AND DISCUSSION

Crystal Structure. To predict the most stable crystal structures of these I−III−Ge_2N_4 compounds, we need to build a series of possible structures. Through replacing the atoms in the wurtzite-based GaN and $ZnGeN_2$ structures, two I−III−Ge_2N_4 structures can be derived, as shown in Figure 2d,e. Other structures, including the kesterite, stannite, and primitive-mixed-CuAu structures of Cu_2ZnSnS_4[12] and the structures of the inorganic compounds with a 1:1:2:4 stoichiometry (can be found in Materials Genome database), have also been considered. The total energy calculations showed that I−III−Ge_2N_4 prefers to crystallize in the structure with a space group of *Pc*, same as the wurtzite-kesterite structure of Cu_2ZnSnS_4 (Li_2ZnGeO_4). The calculated formation energies of these I−III−Ge_2N_4 compounds in the wurtzite-kesterite (*Pc*) and wurtzite-stannite ($Pmn2_1$) structures are listed in Table 1. Obviously, the wurtzite-kesterite structure is at least 100 meV/formula-unit lower in energy than the wurtzite-stannite one, and all other structures have even higher energy than wurtzite-stannite structure, so wurtzite-kesterite is the most stable structure of I−III−Ge_2N_4 among all the structures that we considered.

Table 1. Calculated Formation Energies ΔH_f (in eV/Formula Unit) of I−III−Ge_2N_4 (I = Cu, Ag, Li, Na, K; III = Al, Ga, In) in Wurtzite-Kesterite (*Pc*) and Wurtzite-Stannite ($Pmn2_1$) Structures, and Their Lattice Constants *a*, *b*, and *c* (in Å) in Wurtzite-Kesterite Structure (*Pc*)[a]

	ΔH_f (*Pc*)	ΔH_f ($Pmn2_1$)	*a*	*b*	*c*
$CuAlGe_2N_4$	−2.57	−2.46	6.354	5.437	5.201
$AgAlGe_2N_4$	−1.80	−1.64	6.523	5.543	5.318
$LiAlGe_2N_4$	−4.96	−4.79	6.357	5.443	5.110
$NaAlGe_2N_4$	−3.71	−3.42	6.578	5.563	5.224
$KAlGe_2N_4$	−2.17	−1.75	6.825	5.635	5.383
$CuGaGe_2N_4$	−0.68	−0.43	6.402	5.480	5.249
$AgGaGe_2N_4$	0.08	0.39	6.582	5.586	5.365
$LiGaGe_2N_4$	−3.11	−2.85	6.410	5.474	5.163
$NaGaGe_2N_4$	−1.89	−1.51	6.644	5.594	5.274
$KGaGe_2N_4$	−0.46	0.06	6.923	5.660	5.419
$CuInGe_2N_4$	0.39	0.83	6.687	5.564	5.383
$AgInGe_2N_4$	0.90	1.50	6.871	5.653	5.503
$LiInGe_2N_4$	−1.98	−1.38	6.709	5.569	5.300
$NaInGe_2N_4$	−1.04	−0.19	6.945	5.664	5.413
$KInGe_2N_4$	0.08	1.17	7.200	5.734	5.555

[a]Note that the quaternary wurtzite-derived structure has lower symmetry than the binary wurtzite structure, so it has three lattice constants.

Because the number of possible structures that we considered is limited, the wurtzite-kesterite structure may not be the ground state structure, and these new nitrides I−III−Ge_2N_4 may crystallize in a new quaternary structure that had never been reported. To increase the reliability of our prediction, we used the Crystal structure AnaLYsis by Particle Swarm Optimization (CALYPSO) software[34,35] to search for the most stable structure of I−III−Ge_2N_4 compounds globally. Fifty generations of structures with a population of 30 have been considered. The global search for $LiAlGe_2N_4$ and $LiGaGe_2N_4$ showed that no structure has lower energies than the wurtzite-kesterite structure. This is easy to understand; that is, these quaternary compounds are derived from the wurtzite-structure GaN with a maintained chemical balance, and thus,

DOI: 10.1021/acs.chemmater.5b03536
Chem. Mater. 2015, 27, 7757−7764

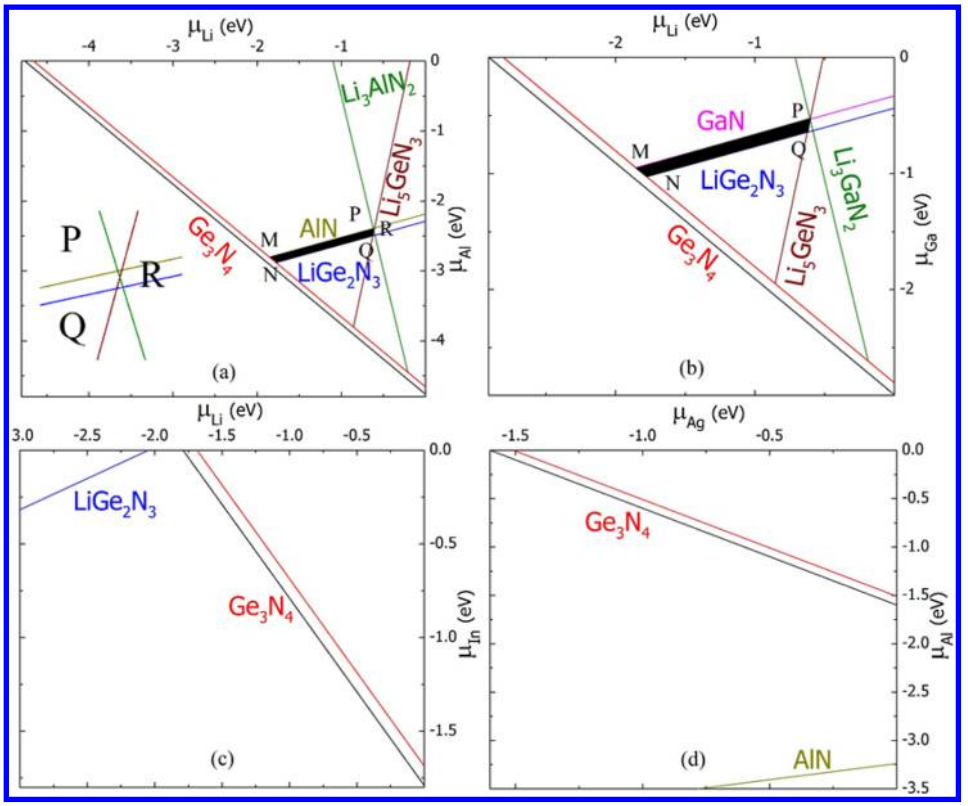

Figure 3. Limit to the regions (black region, if it exists) that stabilize $LiAlGe_2N_4$ (a), $LiGaGe_2N_4$ (b), $LiInGe_2N_4$ (c), and $AgAlGe_2N_4$ (d) in the chemical potential space. Here only slices with $\mu_{Ge} = -0.1$ eV are plotted.

they should be stable in a structure similar to that of GaN. Because the calculated energy of the wurtzite-kesterite structure is the lowest, our following study will be focused on this structure. The calculated lattice constants of I−III−Ge_2N_4 in this structure are also listed in Table 1, which may be compared with the future X-ray diffraction measurement.

Thermodynamic Stability. Although the most stable crystal structure of I−III−Ge_2N_4 (I = Cu, Ag, Li, Na, K; III = Al, Ga, In) is determined from the calculations, it is still a question whether they can be synthesized experimentally or whether they are thermodynamically stable. As the component elements increase, the synthesis of the quaternary nitrides becomes more difficult, because these elements may also form many binary and ternary phases which can compete with the quaternary phase in the synthesis process and coexist in the final products.[11,14,43,44]

In order to predict whether these quaternary nitrides can be synthesized in a certain chemical environment, we introduce the chemical potential of the component elements to describe the chemical environment quantitatively (e.g., μ_{Ge}, μ_{Li}, μ_{Ga} and μ_N of $LiGaGe_2N_4$). When the chemical potential of an element is equal to zero, the element is so rich in the environment that its pure elemental phases can be formed, e.g., $\mu_{Ge} = 0$ means that the bulk Ge in diamond structure can be formed. When the chemical potential is decreased to negative, the element becomes poorer in the environment (the partial pressure becomes lower if it is in the gas phase).

If the quaternary nitride ($LiGaGe_2N_4$ as an example) can be synthesized and is stable, the following thermodynamic equilibrium condition should be reached

$$2\mu_{Ge} + \mu_{Li} + \mu_{Ga} + 4\mu_N = \Delta H_f(LiGaGe_2N_4) \quad (1)$$

where $\Delta H_f(LiGaGe_2N_4)$ is the calculated formation energy of $LiGaGe_2N_4$ (the energy change of the formation reaction from elemental phases to the quaternary compound), which is listed in Table 1. Meanwhile, to avoid the leftover (or coexistence) of elemental phases, Li, Ga, and Ge bulk and N_2 gas, in the final products, the following conditions should be satisfied

$$\mu_{Ge} < 0,\ \mu_{Li} < 0,\ \mu_{Ga} < 0,\ \mu_N < 0 \quad (2)$$

To avoid the formation of the impurity phases such as the binary and ternary nitride compounds, Li_3N, LiN_3, GaN, Ge_3N_4, Li_3GaN_2 and Li_5GeN_3, which may compete with $LiGaGe_2N_4$ during the synthesis process, the following conditions should be satisfied,

$$3\mu_{Li} + \mu_N < \Delta H_f(Li_3N) \quad (3)$$

$$\mu_{Li} + 3\mu_N < \Delta H_f(LiN_3) \quad (4)$$

$$\mu_{Ga} + \mu_N < \Delta H_f(GaN) \quad (5)$$

$$3\mu_{Ge} + 4\mu_N < \Delta H_f(Ge_3N_4) \quad (6)$$

$$3\mu_{Li} + \mu_{Ga} + 2\mu_N < \Delta H_f(Li_3GaN_2) \quad (7)$$

$$5\mu_{Li} + \mu_{Ge} + 3\mu_N < \Delta H_f(Li_5GeN_3) \quad (8)$$

Besides the nitrides shown here, a series of Li−Ga (LiGa, Li_3Ga_2, Li_2Ga, Li_3Ga_7, $LiGa_3$) and Li−Ge (LiGe, Li_9Ge_4, Li_3Ge, $Li_{15}Ge_4$, $Li_{11}Ge_6$, Li_7Ge_2) compounds have also been considered, and they impose more limits on the chemical potentials of Li, Ge, and Ga (μ_{Li}, μ_{Ge}, μ_{Ga}). It has been computationally expensive to determine the crystal structure and calculate the formation energies of all these competing compounds of the quaternary nitrides; however, the recent

DOI: 10.1021/acs.chemmater.5b03536
Chem. Mater. 2015, 27, 7757−7764

development of the Materials Project database has accelerated this process significantly.[42] The calculated formation energies of all the binary and ternary compounds are listed in Tables S1 and S2.

If there exists a certain chemical potential (μ_{Ge}, μ_{Li}, μ_{Ga}, μ_N) that can satisfy all these thermodynamic conditions (1−8), a single-phase sample of the quaternary nitride can be synthesized without the coexistence of any impurity phases in the environment corresponding to this chemical potential. Therefore, we can predict whether $LiGaGe_2N_4$ can be synthesized by solving the mathematical equation/inequation arrays and determining the range of (μ_{Ge}, μ_{Li}, μ_{Ga}, μ_N).[11,45] Because of Equation 1, only three of the variables (μ_{Ge}, μ_{Li}, μ_{Ga}, μ_N) are independent, and we can choose μ_{Ge}, μ_{Li}, μ_{Ga} as the variables (μ_N can be derived). The solution of these inequations falls in a region in the three-dimensional (μ_{Ge}, μ_{Li}, μ_{Ga}) space. In Figure 3b, the region in the $\mu_{Ge} = -0.1$ eV plane is plotted for $LiGaGe_2N_4$. The black area shows the region where (μ_{Ge}, μ_{Li}, μ_{Ga}, μ_N) satisfy all the conditions, and the lines are corresponding to the limit imposed by the binary and ternary compounds (e.g., Ge_3N_4 (red line) and $LiGe_2N_3$ (blue line)). The existence of this region indicates that $LiGaGe_2N_4$ can be synthesized from the thermodynamic point of view. On the other hand, the region is quite narrow for μ_{Ga}, indicating that the control of the Ga chemical potential (richness) is very important for synthesizing single-phase and high-quality $LiGaGe_2N_4$ samples. The strictest limit results from GaN and $LiGe_2N_3$, because the energy cost for the phase separation $LiGaGe_2N_4 \rightarrow GaN+LiGe_2N_3$ is small.

Similarly for $LiAlGe_2N_4$, there exists a region in the chemical potential space that satisfies all the thermodynamic conditions, as shown in Figure 3a, so it is possible to synthesize $LiAlGe_2N_4$. The control of Al richness is very important in the synthesis, because the energy cost of the phase separation $LiAlGe_2N_4 \rightarrow GaN+LiGe_2N_3$ is small too.

In contrast to $LiGaGe_2N_4$ and $LiAlGe_2N_4$, all other quaternary nitrides (I−III−Ge_2N_4 (I = Cu, Ag, Na, K; III = Al, Ga, In) and $LiInGe_2N_4$) do not have a region in the chemical potential space that satisfy all the thermodynamic conditions. Five of them have positive formation energies (listed in Table 1), indicating that the elements prefer to stay at their elemental phases, rather than bind in the quaternary lattice, so they can not satisfy the eq (1) and ineq (2). Other quaternary nitrides have negative formation energies relative to the elemental phases, but the limits from the binary and ternary compounds preclude the existence of a black region, as shown in Figure 3c,d for $LiInGe_2N_4$ and $AgAlGe_2N_4$, respectively. In the $\mu_{Ge} = -0.1$ eV plane, either $LiGe_2N_3$ or Ge_3N_4 can be formed no matter where the chemical potential (μ_{Li}, μ_{Ga}) is located, so $LiGe_2N_3$ or Ge_3N_4 always exist in the samples, and single-phase quaternary $LiInGe_2N_4$ cannot be synthesized. Similarly, AlN or Ge_3N_4 always exist in Figure 3d, so single-phase $AgAlGe_2N_4$ cannot be synthesized either.

The disappearance of a stable region in the chemical potential space can also be simply ascribed to that the quaternary nitrides are unstable with respect to some phase-separation reactions. For example, $CuGaGe_2N_4$ does not have a stable region due to the constraint imposed by Ge_3N_4, Cu_3N, and GaN. This kind of constraint can be described by the following phase-separation reaction

$$3CuGaGe_2N_4 \rightarrow 2Ge_3N_4 + 3GaN + Cu_3N \quad (9)$$

which is an exothermic reaction because the calculated energy change (ΔE, shown in Table 2.) is negative (i.e., this reaction can proceed spontaneously). This causes the disappearance of the stable region of $CuGaGe_2N_4$. A series of the phase-separation reactions of the unstable quaternary nitrides, and their energy changes are listed in Table 2.

Table 2. Phase-Separation Reactions of I−III−Ge_2N_4 (I = Cu, Ag, Na, K; III = Al, Ga, In) and $LiInGe_2N_4$, and Their Energy Changes ΔE (in eV)

quaternary phase	phase-separation reaction	ΔE
$CuGaGe_2N_4$	$3CuGaGe_2N_4 \rightarrow 2Ge_3N_4 + 3GaN + Cu_3N$	−1.67
$NaGaGe_2N_4$	$NaGaGe_2N_4 \rightarrow NaGe_2N_3 + GaN$	−0.40
$KGaGe_2N_4$	$3KGaGe_2N_4 \rightarrow 2Ge_3N_4 + 3GaN + K_3N$	−0.42
$CuAlGe_2N_4$	$3CuAlGe_2N_4 \rightarrow 2Ge_3N_4 + 3AlN + Cu_3N$	−1.56
$NaAlGe_2N_4$	$NaAlGe_2N_4 \rightarrow NaGe_2N_3 + AlN$	−0.45
$KAlGe_2N_4$	$3KAlGe_2N_4 \rightarrow 2Ge_3N_4 + 3AlN + K_3N$	−0.87
$NaInGe_2N_4$	$NaInGe_2N_4 \rightarrow NaGe_2N_3 + InN$	−0.13

In summary, among all these quaternary nitrides we designed, only two of them are thermodynamically stable and can be synthesized experimentally without impurity phases. They are $LiAlGe_2N_4$ and $LiGaGe_2N_4$. Due to the small stable region in the chemical potential spaces, it is necessary to control the richness of the component elements precisely in the synthesis process.

The element abundance of the source materials in Earth's crust is 17 ppm for Li, 19 ppm for Ga, 82 000 ppm for Al, 1.4 ppm for Ge, and 20 ppm for N, all of which are more abundant than In (0.16 ppm).[46] A possible strategy for their growth would be Metalorganic Chemical Vapor Deposition (MOCVD), despite that the available gaseous precursors of Li is limited. Alternatively, sintering the precursor elements or binary nitrides into the $LiAlGe_2N_4$ ($LiGaGe_2N_4$) target and then sputtering into films would be another possible way to make them into thin films, and NH_3 or N_2 atmosphere should be provided to overcome possible N loss during the sputtering process. Special attention should be paid to substrate temperature or partial pressure during the MOCVD or sputtering process in order to avoid the decomposition of this quaternary compound into binary or ternary side products.

Electronic and Optical Properties of $LiAlGe_2N_4$ and $LiGaGe_2N_4$. Because $LiAlGe_2N_4$ and $LiGaGe_2N_4$ are thermodynamically stable, we study their electronic and optical properties to see whether they are suitable for optoelectronic applications. The calculated band structure and density of states (DOS) of $LiAlGe_2N_4$ and $LiGaGe_2N_4$ are shown in Figure 4. Evidently, both $LiAlGe_2N_4$ and $LiGaGe_2N_4$ have direct band gaps, with the valence band maximum (VBM) and the conduction band minimum (CBM) both located at Γ point. The gap of $LiAlGe_2N_4$ is 4.36 eV, larger than that of $LiGaGe_2N_4$ (3.74 eV). The direct nature of the band gaps can be considered as derived from GaN, which also has a direct band gap (3.4 eV) at Γ point, indicating that the crystal structure similarity (as shown in Figure 2) also leads to the electronic band structure similarity. Compared to binary GaN and ternary $ZnGeN_2$, the quaternary $LiAlGe_2N_4$ and $LiGaGe_2N_4$ have larger band gaps, which is in contrast with the monotonic band gap decrease in the ZnS → $CuGaS_2$ → Cu_2ZnGeS_4 (or Cu_2ZnSnS_4). This can be understood

DOI: 10.1021/acs.chemmater.5b03536
Chem. Mater. 2015, 27, 7757−7764

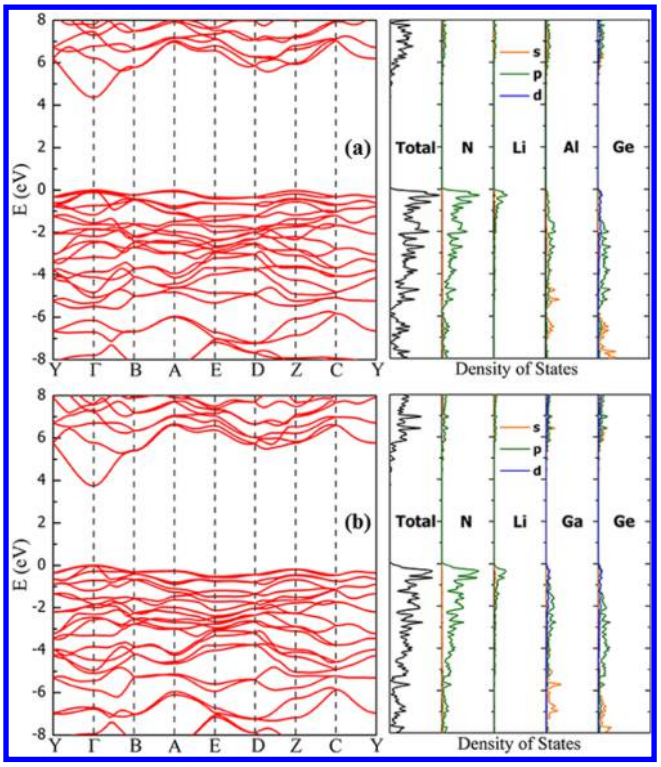

Figure 4. Band structure and density of states of $LiAlGe_2N_4$ (a) and $LiGaGe_2N_4$ (b), calculated using the hybrid functional HSE.

according to the following analysis of the calculated DOS and band alignment.

The total and partial DOS of $LiAlGe_2N_4$ and $LiGaGe_2N_4$ are shown in Figure 4. The top of the valence bands of $LiGaGe_2N_4$ is composed mainly of the N 2p states, weakly hybridized with the Ge 4p, Ge 3d, Ga 4p, Ga 3d, and Li 2p states, whereas the bottom of the conduction band is composed mainly of the antibonding states of the hybridization between Ge 4s, Ga 4s, and N 2s states. Because the N 2p orbitals are localized and their hybridization with other orbitals are weak in these nitrides, the highest valence band has a small dispersion, in contrast with the large dispersion of the lowest conduction band, which is composed mainly of the more delocalized Ge 4s, Ga 4s, and N 2s orbitals.

The band component of $LiAlGe_2N_4$ is similar to that of $LiGaGe_2N_4$, but the top of the valence bands has only N 2p, Ge 4p, Ge 3d, Al 3p, and Li 2p component, and the bottom of the conduction band has only Ge 4s and N 2s component. Therefore, both $LiAlGe_2N_4$ and $LiGaGe_2N_4$ can be considered as semiconductors with typical s−p band gaps, similar to GaN or other III−V semiconductors with s−p band gaps. The similar band component indicates that continuous and flexible band structure engineering may be possible through forming the heterostructures between the quaternary nitrides and GaN.

The band gaps of $LiAlGe_2N_4$ and $LiGaGe_2N_4$ are slightly larger than that of GaN, which can be understood according to the above analysis on the band component. In the top valence bands of GaN, the N 2p states are weakly hybridized with Ga 3d and 4p states which shifts the valence bands (antibonding state) up and decreases the band gap, but after the mutation from GaN to $LiAlGe_2N_4$ or $LiGaGe_2N_4$, the Ga component is largely decreased, and the hybridization becomes even weaker, so the valence bands drop down relative to that of GaN. This is supported by our calculated band offsets, as shown in Figure 5.

The VBM of $LiGaGe_2N_4$ is 0.48 eV lower than that of GaN, and the VBM of $LiAlGe_2N_4$ is even lower, 0.71 eV lower than that of GaN, because all the Ga component is removed.

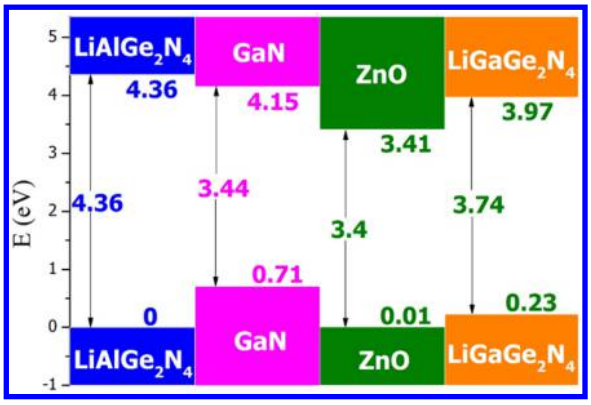

Figure 5. Calculated band alignment for $LiAlGe_2N_4$, GaN, ZnO, and $LiGaGe_2N_4$. The VBM energy level of $LiAlGe_2N_4$ is set to zero. The ZnO/GaN valence band offset of 0.7 eV is collected from ref 47.

Comparing the CBM states of GaN and $LiGaGe_2N_4$, Ge 4s level is lower than Ga 4s level,[12] which shifts the CBM level down, but the Li 2s level is much higher than Ga 4s level, which shifts the CBM level up, so the two contributions canceled each other. Because the Ge:Li ratio is 2:1, the final result is that the CBM level of $LiGaGe_2N_4$ is slightly shifted down, 0.18 eV lower than that of GaN (see Figure 5). Because Al 3s level is also higher than Ga 4s level, the CBM level of $LiAlGe_2N_4$ is slightly shifted up, 0.21 eV higher than that of GaN. Considering both the shifts of VBM and CBM levels, we can understand the band gap increases of the quaternary compounds.

Because the band gaps of $LiGaGe_2N_4$ and $LiAlGe_2N_4$ are both direct, a strong absorption of the UV light is expected, which is confirmed by our calculated absorption spectra and dielectric constants in Figure 6. The absorption coefficient increases rapidly to the order of 10^5 cm^{-1} as the photon energy is above the direct band gaps, indicating that the optical transition between the s−p band gaps is very strong. On the other hand, the valence bands of both compounds have a high density of states (peak) just below the VBM level, which also

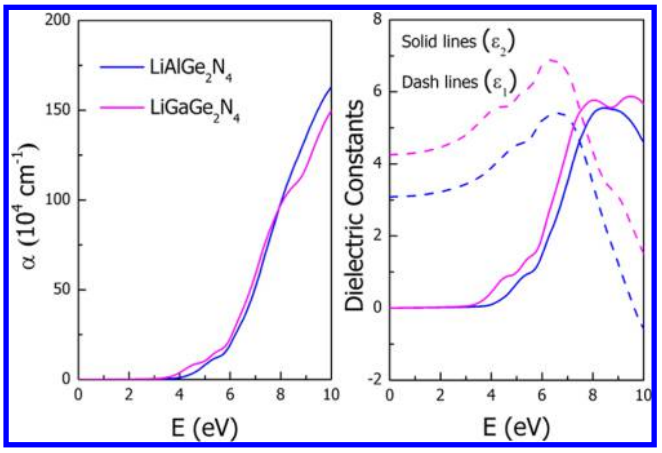

Figure 6. Calculated optical absorption coefficient (α) and dielectric constants of $LiAlGe_2N_4$ (blue) and $LiGaGe_2N_4$ (magenta), using the hybrid functional HSE.

DOI: 10.1021/acs.chemmater.5b03536
Chem. Mater. 2015, 27, 7757−7764

contributes to the rapid increase of the absorption coefficient. The strong absorption of the UV light makes these quaternary nitrides very competitive for the UV light detector.

As shown in Figure 5, these quaternary nitrides have their valence band edge levels as low as that of ZnO (the VBM level of $LiAlGe_2N_4$ is even lower than that of ZnO), and their CBM levels can also be shifted above or below that of GaN, indicating that the element mutation provides an efficient method for manipulating the band edge positions. Furthermore, the lattice constants of $LiGaGe_2N_4$ and $LiAlGe_2N_4$ are well matched to GaN and ZnO, with a lattice mismatch less than 3%, as shown in Table 1 (the lattice constants of GaN and ZnO in the same supercell as that in Figure 2 are a = 6.380 Å, b = 5.525 Å, c = 5.189 Å and a = 6.506 Å, b = 5.634 Å, c = 5.210 Å respectively). Considering that the crystal structure and electronic structure (band component) are both similar to GaN (a natural consequence of the cation-mutation), we expect that various heterostructures (superlattice, core−shell quantum dots, etc.) based on $LiAlGe_2N_4$, $LiGaGe_2N_4$ and GaN (or even ZnO) can be readily fabricated, and flexible and continuous band structure engineering can be achieved in these lattice matched heterostructures, which may give rise to various applications in UV optoelectronic devices. Experimental synthesis of $LiAlGe_2N_4$ and $LiGaGe_2N_4$ is called for.

IV. CONCLUSIONS

Through cation-mutation in GaN, we found for the first time that two quaternary nitride semiconductors ($LiAlGe_2N_4$ and $LiGaGe_2N_4$) can be thermodynamically stable, whereas other quaternary nitrides I−III−Ge_2N_4 (I = Cu, Ag, Li, Na, K; III = Al, Ga, In) are not stable with respect to the phase separation into binary or ternary nitrides. Our results explain why quaternary nitrides had never been synthesized experimentally and indicate that the control of the Ga (Al) richness in the environment is critical for synthesizing single-phase $LiGaGe_2N_4$ ($LiAlGe_2N_4$). The calculated band structure and optical absorption spectra showed that the new quaternary nitrides ($LiAlGe_2N_4$ and $LiGaGe_2N_4$) are direct-band gap semiconductors with strong absorption of ultraviolet light. Furthermore, they are both lattice-matched to GaN or ZnO, and their valence band edge levels can be lower than that of ZnO; however, their conduction band edge levels are higher than that of GaN, and therefore, flexible band structure engineering can be achieved in the lattice-matched GaN/ $LiAlGe_2N_4$/ $LiGaGe_2N_4$ superlattices or heterostructures, which may work as high-performance ultraviolet optoelectronic devices.

■ ASSOCIATED CONTENT

Supporting Information

The Supporting Information is available free of charge on the ACS Publications website at DOI: 10.1021/acs.chemmater.5b03536.

Space group and formation energies of all considered secondary phases (PDF)

■ AUTHOR INFORMATION

Corresponding Author

*E-mail for S.C.: chensy@ee.ecnu.edu.cn.

Notes

The authors declare no competing financial interest.

■ ACKNOWLEDGMENTS

We thank Prof. Jiang Tang for the helpful discussion about the viable synthesis strategy. The work was supported by the National Natural Science Foundation of China (grant no. 91233121, 61125403), Shanghai Rising-Star Program (grant no. 14QA1401500), Special Funds for Major State Basic Research (grant no. 2012CB921401, 2014CB921104), PCSIRT and the computer center of ECNU. P.N. is supported by the National Science Foundation and the Resnick Sustainability Institute at Caltech.

■ REFERENCES

(1) Nakamura, S. The Roles of Structural Imperfections in InGaN-Based Blue Light-Emitting Diodes and Laser Diodes. *Science* **1998**, *281*, 956−961.

(2) Du, M.-H.; Limpijumnong, S.; Zhang, S. B. Hydrogen-Mediated Nitrogen Clustering in Dilute III-V Nitrides. *Phys. Rev. Lett.* **2006**, *97*, 075503.

(3) Taniyasu, Y.; Kasu, M.; Makimoto, T. An aluminium nitride light-emitting diode with a wavelength of 210 nanometres. *Nature* **2006**, *441*, 325−328.

(4) Kobayashi, Y.; Yamauchi, Y.; Kobayashi, N. K. Structural and optical properties of AlGaInN/GaN grown by MOVPE. *Jpn. J. Appl. Phys.* **2003**, *42*, 2300−2304.

(5) Mánuel, J. M.; Morales, F. M.; Lozano, J. G.; González, D.; García, R.; Lim, T.; Kirste, L.; Aidam, R.; Ambacher, O. Structural and compositional homogeneity of InAlN epitaxial layers nearly lattice-matched to GaN. *Acta Mater.* **2010**, *58*, 4120−4125.

(6) Mánuel, J. M.; Koch, C. T.; ÖzdÖL, V. B.; Sigle, W.; Van Aken, P. A.; GarcÍA, R.; Morales, F. M. Inline electron holography and VEELS for the measurement of strain in ternary and quaternary (In,Al,Ga)N alloyed thin films and its effect on bandgap energy. *J. Microsc.* **2015**, DOI: 10.1111/jmi.12312.

(7) Morales, F. M.; Mánuel, J. M.; García, R.; Reuters, B.; Kalisch, H.; Vescan, A. Evaluation of interpolations of InN, AlN and GaN lattice and elastic constants for their ternary and quaternary alloys. *J. Phys. D: Appl. Phys.* **2013**, *46*, 245502.

(8) Khan, A.; Balakrishnan, K.; Katona, T. Ultraviolet light-emitting diodes based on group three nitrides. *Nat. Photonics* **2008**, *2*, 77−84.

(9) Kneissl, M.; Kolbe, T.; Chua, C.; Kueller, V.; Lobo, N.; Stellmach, J.; Knauer, A.; Rodriguez, H.; Einfeldt, S.; Yang, Z.; Johnson, N. M.; Weyers, M. Advances in group III-nitride-based deep UV light-emitting diode technology. *Semicond. Sci. Technol.* **2011**, *26*, 014036.

(10) Moustakas, T. D.; Singh, R.; Korakakis, D.; Doppalapudi, D.; Ng, H. M.; Sampath, A.; Iliopoulos, E.; Misra, M. Phase separation and atomic ordering in AlGaInN alloys. *MRS Online Proc. Libr.* **1998**, *482*, 193−204.

(11) Wang, C. C.; Chen, S. Y.; Yang, J. H.; Lang, L.; Xiang, H. J.; Gong, X. G.; Walsh, A.; Wei, S. H. Design of I-2-II-IV-VI4 Semiconductors through Element Substitution: The Thermodynamic Stability Limit and Chemical Trend. *Chem. Mater.* **2014**, *26*, 3411−3417.

(12) Chen, S.; Gong, X. G.; Walsh, A.; Wei, S.-H. Electronic structure and stability of quaternary chalcogenide semiconductors derived from cation cross-substitution of II-VI and I-III-VI2 compounds. *Phys. Rev. B: Condens. Matter Mater. Phys.* **2009**, *79*, 165211.

(13) Todorov, T. K.; Tang, J.; Bag, S.; Gunawan, O.; Gokmen, T.; Zhu, Y.; Mitzi, D. B. Beyond 11% Efficiency: Characteristics of State-of-the-Art Cu2ZnSn(S,Se)(4) Solar Cells. *Adv. Energy Mater.* **2013**, *3*, 34−38.

(14) Chen, S. Y.; Walsh, A.; Gong, X. G.; Wei, S. H. Classification of Lattice Defects in the Kesterite Cu2ZnSnS4 and Cu2ZnSnSe4 Earth-Abundant Solar Cell Absorbers. *Adv. Mater.* **2013**, *25*, 1522−1539.

(15) Graetzel, M.; Janssen, R. A. J.; Mitzi, D. B.; Sargent, E. H. Materials interface engineering for solution-processed photovoltaics. *Nature* **2012**, *488*, 304−312.

DOI: 10.1021/acs.chemmater.5b03536
Chem. Mater. 2015, 27, 7757−7764

(16) Ford, G. M.; Guo, Q. J.; Agrawal, R.; Hillhouse, H. W. Earth Abundant Element Cu2Zn(Sn1-xGex)S-4 Nanocrystals for Tunable Band Gap Solar Cells: 6.8% Efficient Device Fabrication. *Chem. Mater.* **2011**, *23*, 2626−2629.
(17) Nagaoka, A.; Miyake, H.; Taniyama, T.; Kakimoto, K.; Nose, Y.; Scarpulla, M. A.; Yoshino, K. Effects of sodium on electrical properties in Cu2ZnSnS4 single crystal. *Appl. Phys. Lett.* **2014**, *104*, 152101.
(18) Pamplin, B. R. Super-Cell Structure of Semiconductors. *Nature* **1960**, *188*, 136−137.
(19) Goodman, C. H. L. The prediction of semiconducting properties in inorganic compounds. *J. Phys. Chem. Solids* **1958**, *6*, 305−314.
(20) Fan, F. J.; Wu, L.; Yu, S. H. Energetic I-III-VI2 and I-2-II-IV-VI4 nanocrystals: synthesis, photovoltaic and thermoelectric applications. *Energy Environ. Sci.* **2014**, *7*, 190−208.
(21) Fan, F. J.; Yu, B.; Wang, Y. X.; Zhu, Y. L.; Liu, X. J.; Yu, S. H.; Ren, Z. F. Colloidal Synthesis of Cu2CdSnSe4 Nanocrystals and Hot-Pressing to Enhance the Thermoelectric Figure-of-Merit. *J. Am. Chem. Soc.* **2011**, *133*, 15910−15913.
(22) Tsuji, I.; Shimodaira, Y.; Kato, H.; Kobayashi, H.; Kudo, A. Novel Stannite-type Complex Sulfide Photocatalysts A(2)(I)-Zn-A(IV)-S-4 (A(I) = Cu and Ag; A(IV) = Sn and Ge) for Hydrogen Evolution under Visible-Light Irradiation. *Chem. Mater.* **2010**, *22*, 1402−1409.
(23) Todorov, T. K.; Reuter, K. B.; Mitzi, D. B. High-Efficiency Solar Cell with Earth-Abundant Liquid-Processed Absorber. *Adv. Mater.* **2010**, *22*, E156−E159.
(24) Shavel, A.; Arbiol, J.; Cabot, A. Synthesis of Quaternary Chalcogenide Nanocrystals: Stannite Cu2ZnxSnySe1+x+2y. *J. Am. Chem. Soc.* **2010**, *132*, 4514−4515.
(25) Ahn, S.; Jung, S.; Gwak, J.; Cho, A.; Shin, K.; Yoon, K.; Park, D.; Cheong, H.; Yun, J. H. Determination of band gap energy (Eg) of Cu2ZnSnSe4 thin films: On the discrepancies of reported band gap values. *Appl. Phys. Lett.* **2010**, *97*, 021905.
(26) Narang, P.; Chen, S.; Coronel, N. C.; Gul, S.; Yano, J.; Wang, L.-W.; Lewis, N. S.; Atwater, H. A. Bandgap Tunability in Zn(Sn,Ge)N2 Semiconductor Alloys. *Adv. Mater.* **2014**, *26*, 1235−1241.
(27) Chen, S.; Narang, P.; Atwater, H. A.; Wang, L.-W. Phase Stability and Defect Physics of a Ternary ZnSnN2 Semiconductor: First Principles Insights. *Adv. Mater.* **2014**, *26*, 311−315.
(28) Liu, B. W.; Zhang, M. J.; Zhao, Z. Y.; Zeng, H. Y.; Zheng, F. K.; Guo, G. C.; Huang, J. S. Synthesis, structure, and optical properties of the quaternary diamond-like compounds I-2-II-IV-VI4 (I = Cu; II = Mg; IV = Si, Ge; VI = S, Se). *J. Solid State Chem.* **2013**, *204*, 251−256.
(29) Washio, T.; Shinji, T.; Tajima, S.; Fukano, T.; Motohiro, T.; Jimbo, K.; Katagiri, H. 6% Efficiency Cu2ZnSnS4-based thin film solar cells using oxide precursors by open atmosphere type CVD. *J. Mater. Chem.* **2012**, *22*, 4021−4024.
(30) Wang, X.; Li, J.; Zhao, Z.; Huang, S.; Xie, W. Crystal structure and electronic structure of quaternary semiconductors Cu2ZnTiSe4 and Cu2ZnTiS4 for solar cell absorber. *J. Appl. Phys.* **2012**, *112*, 023701.
(31) Shang, M.; Li, G.; Yang, D.; Kang, X.; Peng, C.; Lin, J. Luminescence properties of Mn2+-doped Li2ZnGeO4 as an efficient green phosphor for field-emission displays with high color purity. *Dalton Trans.* **2012**, *41*, 8861−8868.
(32) Levcenco, S.; Dumcenco, D.; Huang, Y. S.; Tiong, K. K.; Du, C. H. Anisotropy of the spectroscopy properties of the wurtz-stannite Cu2ZnGeS4 single crystals. *Opt. Mater.* **2011**, *34*, 183−188.
(33) Chen, S.; Walsh, A.; Luo, Y.; Yang, J.-H.; Gong, X. G.; Wei, S.-H. Wurtzite-derived polytypes of kesterite and stannite quaternary chalcogenide semiconductors. *Phys. Rev. B: Condens. Matter Mater. Phys.* **2010**, *82*, 195203.
(34) Wang, Y. C.; Lv, J.; Zhu, L.; Ma, Y. M. CALYPSO: A method for crystal structure prediction. *Comput. Phys. Commun.* **2012**, *183*, 2063−2070.
(35) Wang, Y.; Lv, J.; Zhu, L.; Ma, Y. Crystal structure prediction via particle-swarm optimization. *Phys. Rev. B: Condens. Matter Mater. Phys.* **2010**, *82*, 094116.
(36) Kresse, G.; Furthmuller, J. Efficiency of ab-initio total energy calculations for metals and semiconductors using a plane-wave basis set. *Comput. Mater. Sci.* **1996**, *6*, 15−50.
(37) Kresse, G.; Furthmuller, J. Efficient iterative schemes for ab initio total-energy calculations using a plane-wave basis set. *Phys. Rev. B: Condens. Matter Mater. Phys.* **1996**, *54*, 11169−11186.
(38) Perdew, J. P.; Burke, K.; Ernzerhof, M. Generalized gradient approximation made simple. *Phys. Rev. Lett.* **1996**, *77*, 3865−3868.
(39) Chen, S.; Gong, X. G.; Walsh, A.; Wei, S.-H. Crystal and electronic band structure of Cu2ZnSnX4 (X = S and Se) photovoltaic absorbers: First-principles insights. *Appl. Phys. Lett.* **2009**, *94*, 041903.
(40) Lyons, J. L.; Janotti, A.; Van de Walle, C. G. Carbon impurities and the yellow luminescence in GaN. *Appl. Phys. Lett.* **2010**, *97*, 152108.
(41) Monkhorst, H. J.; Pack, J. D. Special points for Brillouin-zone integrations. *Phys. Rev. B* **1976**, *13*, 5188−5192.
(42) Jain, A.; Ong, S. P.; Hautier, G.; Chen, W.; Richards, W. D.; Dacek, S.; Cholia, S.; Gunter, D.; Skinner, D.; Ceder, G.; Persson, K. A. Commentary: The Materials Project: A materials genome approach to accelerating materials innovation. *APL Mater.* **2013**, *1*, 011002.
(43) Chen, S.; Yang, J.-H.; Gong, X. G.; Walsh, A.; Wei, S.-H. Intrinsic point defects and complexes in the quaternary kesterite semiconductor Cu2ZnSnS4. *Phys. Rev. B: Condens. Matter Mater. Phys.* **2010**, *81*, 245204.
(44) Chen, S.; Gong, X. G.; Walsh, A.; Wei, S.-H. Defect physics of the kesterite thin-film solar cell absorber Cu2ZnSnS4. *Appl. Phys. Lett.* **2010**, *96*, 021902.
(45) Buckeridge, J.; Scanlon, D. O.; Walsh, A.; Catlow, C. R. A. Automated procedure to determine the thermodynamic stability of a material and the range of chemical potentials necessary for its formation relative to competing phases and compounds. *Comput. Phys. Commun.* **2014**, *185*, 330−338.
(46) Abundance in Earth's crust: Periodicity. http://www.webelements.com/periodicity/abundance_crust/.
(47) Huda, M. N.; Yan, Y.; Wei, S.-H.; Al-Jassim, M. M. Electronic structure of ZnO:GaN compounds: Asymmetric bandgap engineering. *Phys. Rev. B: Condens. Matter Mater. Phys.* **2008**, *78*, 195204.

DOI: 10.1021/acs.chemmater.5b03536
Chem. Mater. 2015, 27, 7757−7764